Benjamin Prek, Marta Počkaj, Willi Kantlehner and Branko Stanovnik*

Thermal metal-free [2+2] cycloaddition of acetylenedicarboxylates to polysubstituted butadienes

https://doi.org/10.1515/znb-2018-0052
Received April 18, 2018; accepted May 6, 2018

Abstract: The thermal metal-free [2+2] cycloadditions of electron-poor acetylenes to some polysubstituted systems with conjugated double bonds (polysubstituted butadienes) are described.

Keywords: dimethyl 2-phenylpyridine-3,6-dicarboxylate; electron-poor acetylenes; polysubstituted butadienes; thermal metal-free [2+2] cycloaddition.

1 Introduction

[2+2] Cycloadditions of electron-poor acetylenes to push–pull systems, such as 3-(dimethylamino)propenoates, acyclic and cyclic enamines, and some heterocyclic enaminones, have been described recently [1]. Polysubstituted butadienes have been prepared by microwave-assisted [2+2] cycloadditions of enaminones to electron-poor acetylenes [2, 3]. Polysubstituted aminobutadienes prepared by this procedure are suitable for the preparation of polysubstituted pyridine derivatives. They also represent a group of isomeric intermediates in regard to the aminobutadienes prepared via the Michael addition in Bohlmann–Rahtz synthesis of pyridine derivatives [4, 5]. On this basis, a simple metal-free synthesis of 2-alkyl-, 2-cycloalkyl-, 2-aryl-, and 2-heteroaryl-substituted pyridine-3,4-dicarboxylates and their *N*-oxides has been developed [6]. The electron-poor propyne iminium triflates, prepared from 3-trifloxypropene iminium triflates by elimination of triflic acid, underwent [2+2] and [2+4] cycloadditions with enamines [7]. Their reactivity toward imines has been also reported [8, 9]. Recently, we reported on a simple one-pot metal-free synthesis of 2,4,5-trisubstituted pyridine derivatives and their *N*-oxides by [2+2] cycloaddition of propyne iminium salts as electron-poor acetylenes to enaminones as an extension of the research developed in our laboratory [10].

We also recently reported on a simple, metal-free synthesis of polysubstituted benzene derivatives, where *N*,*N*-dimethylacetamide dimethyl acetal (DMADMA) served as the reagent and building block for generating aromatic final products [11]. We have reported on another application of the enaminone system in the synthesis of heterocyclic compounds. We have expanded the DMADMA methodology on aryl- and (hetero) aryl-enaminone systems, as well as on aromatic and heteroaromatic carboxamides, to prepare *N*,*N*,6-trimethyl-4-(substituted)pyridin-2-amines and N^2,N^2,N^4,N^4-tetramethyl-6-(substituted) pyridine-2,4-diamines as the final products [12]. Microwave-assisted [2+2] cycloaddition reactions of 2-amino-3-dimethylaminopropenoates with acetylenecarboxylates furnished highly functionalized 1-amino-4-(dimethylamino)buta-1,3-dienes suitable for preparation of many heterocyclic systems [13].

Recently, we reported on the thermal reactions of cyclic enaminones, derived from cyclic five- and six-membered 1,3-diones and dimethyl acetylenedicarboxylate (DMAD), in which a mixture of two products, ring-expanded products as a result of a [2+2] cycloaddition and Michael adducts, has been produced [14].

In several instances, in the reaction of cyclic enaminones with acetylenedicarboxylates, besides the ring enlarged product as a consequence of [2+2] cycloaddition and Michael type of product, other products have also been isolated, such as tetramer of DMAD [15].

The [2+2] cycloadditions of electron-poor acetylenes to polysubstituted systems with conjugated double bonds (polysubstituted butadienes) have not been described as yet.

***Corresponding author: Branko Stanovnik,** Faculty of Chemistry and Chemical Technology, University of Ljubljana, Večna pot 113, P. O. Box 537, 1000 Ljubljana, Slovenia; and EN_FIST Centre of Excellence, Trg Osvobodilne fronte 3, 1000 Ljubljana, Slovenia, e-mail: branko.stanovnik@fkkt.uni-lj.si
Benjamin Prek and Marta Počkaj: Faculty of Chemistry and Chemical Technology, University of Ljubljana, Večna pot 113, P. O. Box 537, 1000 Ljubljana, Slovenia
Willi Kantlehner: Fakultät Chemie/Organische Chemie, Hochschule Aalen, Beethovenstr. 1, 73430 Aalen, Germany

2 Results and discussion

Several polysubstituted acyclic and cyclic dienes **1a–t** (Fig. 1) were selected. The cycloadditions with acetylenedicarboxylates were carried out in acetonitrile under microwave irradiation (300 W) at various temperatures and prolonged reaction times as the reactivity of dienes is diminished in comparison to enaminones, due to conjugation over four center systems. The reactions were followed by thin-layer chromatography; the reactin components were separated by column chromatography (silicagel-petroleum ether-ethyl acetate) and purified by crystallization.

In general, the diene systems are less reactive in comparison to the push–pull enaminone systems. From the selected butadienes, none has either a primary amino group or primary and secondary amide groups because we have found previously that this kind of substituents do not favor [2+2] cycloadditions. From the compounds presented in Fig. 1, only six of them, that is, compounds **1a–f** (shown in blue in Fig. 1), turned out to be reactive in the [2+2] cycloadditions. We found that **1a–f** react with DMAD or diethyl acetylenedicarboxylate (DEAD) in [2+2] cycladditions to give the corresponding cycloadducts **2a–g**. The products, reaction conditions, and yields are shown in Table 1.

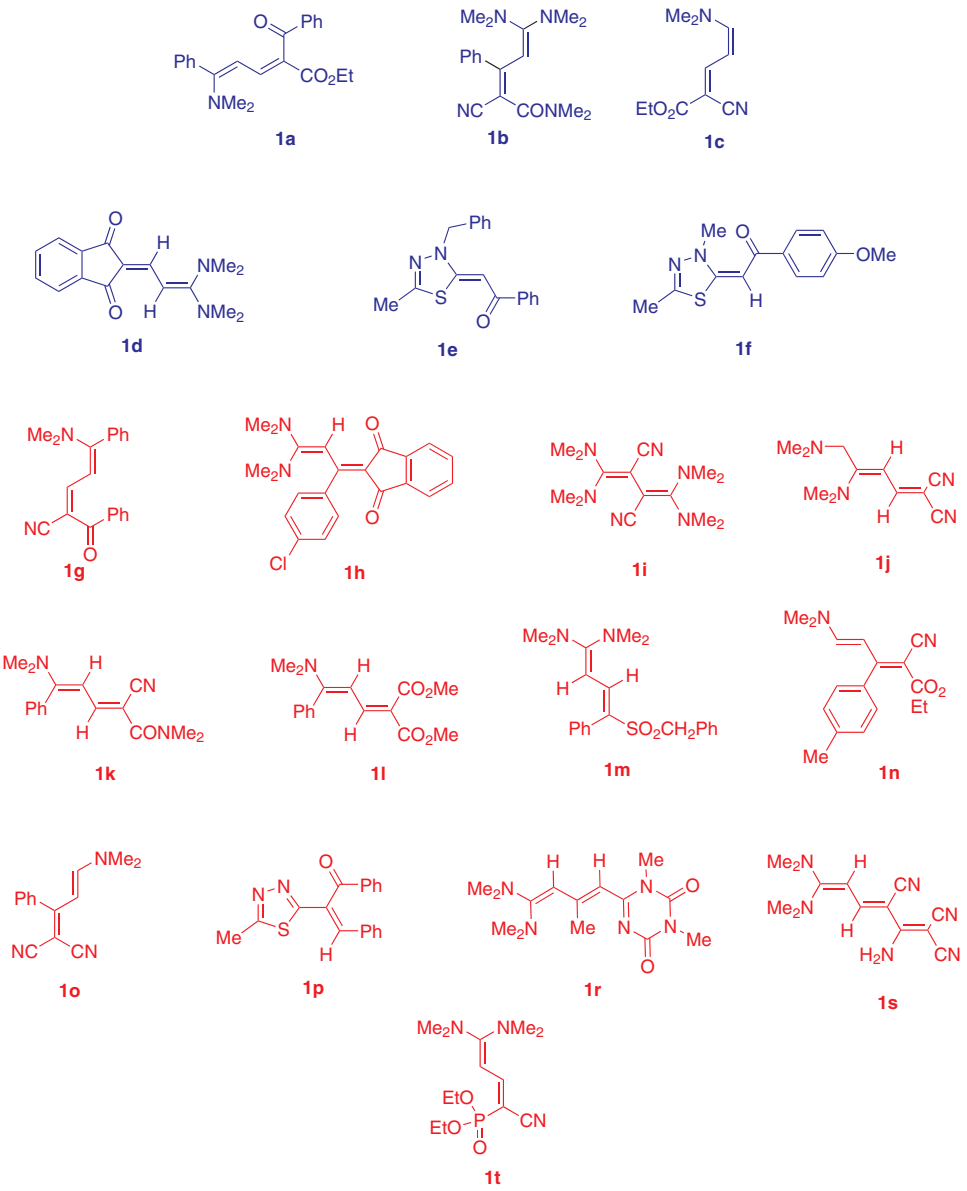

Fig. 1: Compounds selected for thermal [2+2] cycloadditions with acetylenedicarboxylates. For color code, see text.

Table 1: Products of [2+2] cycloadditions.

Starting compound	Product		Reaction time (min)	Temperature (°C)	Yield (%)
1a	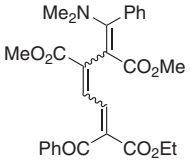	**2a**	30	100	60
1b	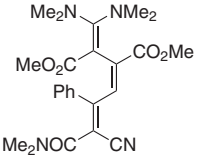	**2b**	15	100	73
1c	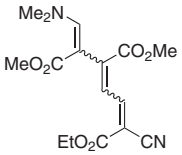	**2c**	40	100	42
1d	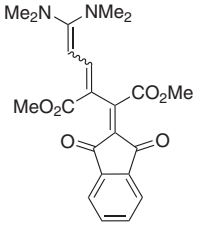	**2d**	10	80	22
1d	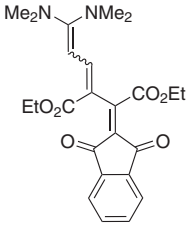	**2e**	20	75	44
1e	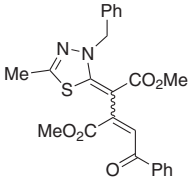	**2f**	15	90	73
1f	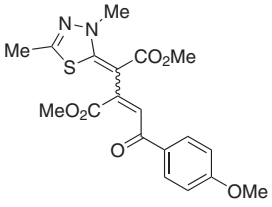	**2g**	15	100	65

Compounds **1g–t** (Fig. 1; shown in red) are not reactive under the same conditions. In these cases, either the unreacted material was recovered or a mixture of various, partially tarry, products were obtained after prolonged reaction time. No attempts were made to separate these mixtures.

The formation of the products can be explained by a two-step mechanism reported in our earlier papers [13, 14]. The initially formed intermediate **a** can be transformed by rotation around the single bond, cyclizing into the sterically favored cyclobutene intermediate **b**, which would produce the final product **c** (Scheme 1) by a conrotatory

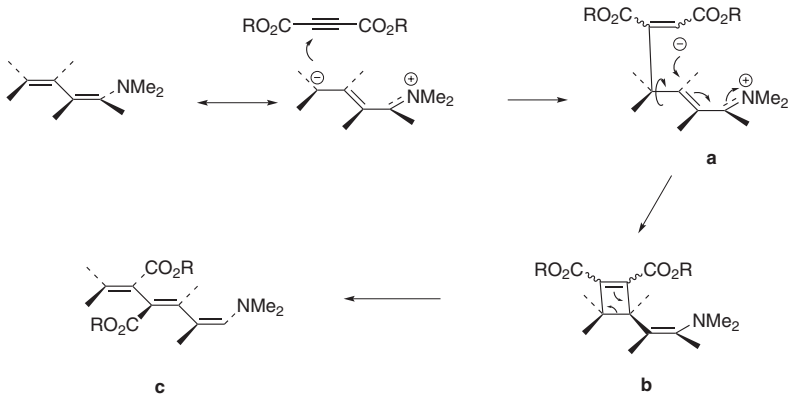

Scheme 1: Two-step mechanism of formation of [2+2] cycloadducts between polysubstituted butadienes and acetylenedicarboxylates.

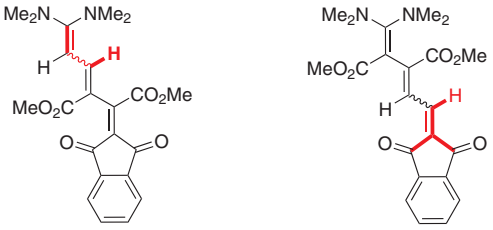

Fig. 2: Two possible cycloadducts from the reaction of **1d** with DMAD.

retro-electrocyclization followed by conratotory ring opening.

The insertion of acetylenediacarboxylate into the double bond of enaminones is clear, whereas the insertion into the diene system is unclear because there are two double bonds. In the case of **1d**, there are two posibilities in which either **2d** or **2d′** (Fig. 2) could be formed because the [2+2] cycloaddition can take place to either of the two double bonds. It turned out that it is possible to differentiate between these two structures based on the proton on the C atom to which two dimethylamino groups attached can be observed; however, in the case of **2d′**, a strong correlation of the vinyl proton with carbonyl C atoms of the indene-1,3-dione structural element should be observed. The heteronuclear multiple bond correlation (HMBC) spectrum (Fig. 3) clearly shows that the structure of the product is **2d**. Analogously, the structures of the other cycloadducts were determined, while the stucture of the cycloadduct **2b** was also confirmed by X-ray structure determination on single crystals (Fig. 4).

The bond lengths of the diene system, seen in the molecular structure of compound **1d** in the crystal (see below), are very informative (Scheme 2) because they clearly show the strong dipolar character of the diene system (represented as **1d′** in Scheme 2) with the negative

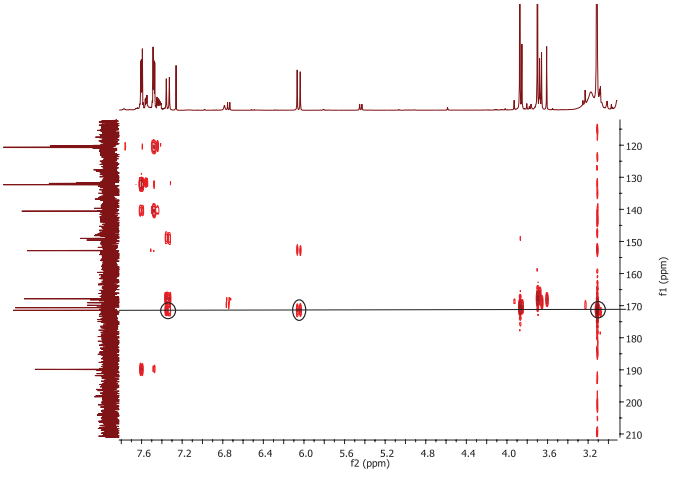

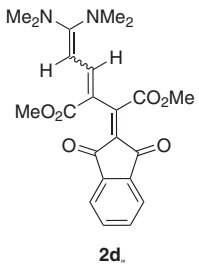

Fig. 3: HMBC spectrum of **2d**.

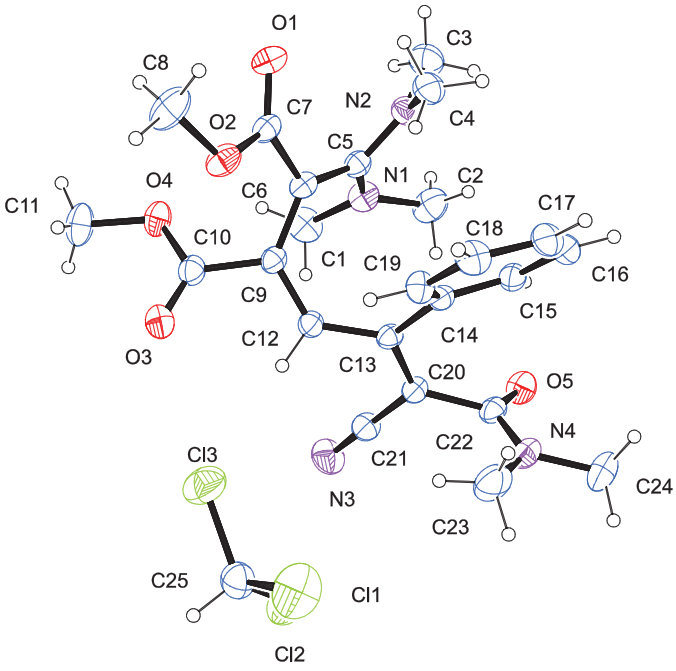

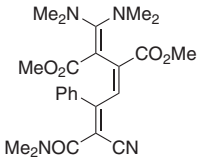

2b

Fig. 4: ORTEP drawing of the molecular structure of compound **2b** in the crystal including the co-crystallized solvate molecule chloroform. Displacement ellipsoids are drawn at the 30% probability level; hydrogen atoms as spheres with arbitrary radii.

part of the dipole on the carbon atom to which cycloaddition of the acetylenedicrboxylate is taking place. This is an additional evidence that speaks in favor of the two-step mechanism of the [2+2] cycloaddition.

Because there are many dienes that do not react in the [2+2] cycloadditions, we tried to make some comparison. All starting compounds have strong electron donors; all reactive compounds, except **1b** and **1c**, contain a carbonyl (ketone) group attached at the electron-rich ene or diene system (Fig. 5).

A comparison of compounds **1e**, **1f**, and **1p** shows that in the case of **1p**, the electron-acceptor group prevents the addition because of steric hindrance. A similar situation is shown in the compound **1h** in which the *p*-chlorophenyl group represents a steric hindrance, and therefore, the cycloaddition is not taking place. A comparison of compounds **1b**, **1k**, and **1l** indicates that in the case of **1k** and **1l**, the push–pull effect is too small and therefore the cycloaddition does not occur, whereas the phenyl group in **1b** does not prevent the cycloaddition (Fig. 5).

In this connection, exact structural information was desirable, which prompted us to determine the crystal and molecular structures of compounds **1b**, **1c**, **1d**, **1g**, **1k**, and **1l**. They furnished the particularly interesting bond lengths of the single and the double bonds of the butadiene structural elements. Figure 6 shows the molecular structures, and Fig. 7 summarizes the respective key bond lengths.

Product **2a** reacted with ammonium acetate upon heating in methanol for several hours to give a mixture of dimethyl 2-phenylpyridine-3,6-dicarboxylate (**3**) and methyl 3-amino-3-phenylacrylate (**4**). Because the reaction was carried out in refluxing methanol, transesterification of the ethyl ester into the methyl ester occurred (Scheme 3).

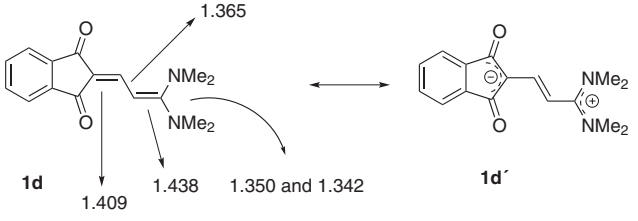

Scheme 2: Resonance structures of **1d** and key bond lengths (in Å) from the single-crystal structure determination.

3 Conclusion

In conclusion, the thermal metal-free [2+2] cycloadditions of electron-poor acetylenes to some polysubstituted systems with conjugated double bonds (polysubstituted butadienes) are described. The structures of the products were determined either by single-crystal X-ray diffraction or by HMBC NMR techniques.

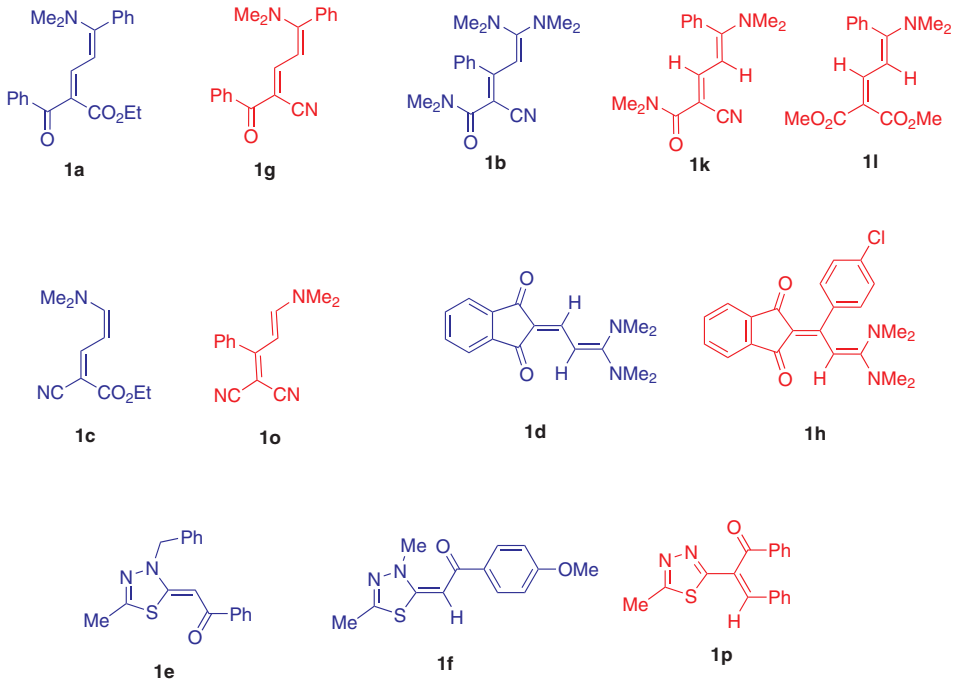

Fig. 5: Side-by-side comparison of compounds reactive in [2+2] cycloadditions (in blue) and compounds unreactive in [2+2] cycloadditions (in red).

4 Experimental section

Melting points were determined on a Stanford Research Systems MPA100 OptiMelt automated melting point system. The NMR spectra were obtained on a Bruker Avance DPX 300 at 300 MHz for ^{1}H and 75.5 MHz for ^{13}C, and on a Bruker Avance III UltraShield 500 Plus at 500 MHz for ^{1}H and 126 MHz for ^{13}C, using $CDCl_3$ and [D_6]DMSO as solvents with Me_4Si as the internal standard. Mass spectra were recorded on a Agilent 6224 Accurate Mass TOF LC/MS spectrometer and IR spectra on a Perkin Elmer Spectrum BX FTIR spectrophotometer. Microanalyses were performed on a Perkin-Elmer CHN Analyzer 2400 II. Column chromatography was performed on silica gel (Fluka, Silica gel 60, particle size 35–70 μm). Starting compounds **1a–t** were prepared according to the procedures reported in the literature: ethyl (2*E*,4*Z*)-2-benzoyl-5-(dimethylamino)-5-phenylpenta-2,4-dienoate (**1a**) [16], (*E*)-2-cyano-5,5-bis(dimethylamino)-*N*,*N*-dimethyl-3-phenylpenta-2,4-dienamide (**1b**) [17], ethyl (2*E*,4*Z*)-2-cyano-5-(dimethylamino)penta-2,4-dienoate (**1c**) [16], 2-(3,3-bis(dimethylamino) allylidene)-1*H*-indene-1,3(2*H*)-dione (**1d**) [17], (*Z*)-2-(3-benzyl-5-methyl-1,3,4-thiadiazol-2(3*H*)-ylidene)-1-phenylethan-1-one (**1e**) [18], (*E*)-2-(3,5-dimethyl-1,3,4-thiadiazol-2(3*H*)-ylidene-1-(4-methoxyphenyl)ethan-1-on (**1f**) [19], (2*Z*,4*Z*)-2-benzoyl-5-(dimethylamino)-5-phenylpenta-2,4-dienenitrile (**1g**) [16], 2-(1-(4-chlorophenyl)-3,3-bis(dimethylamino) allylidene-1*H*-indene-1,3(2*H*)-dione (**1h**) [20], 2,3-bis(bis-(dimethyl-amino)methylene)succinonitrile (**1i**) [20], (*Z*)-2-(3,4-bis(dimethylamino)but-2-en-1-ylidene)malononitrile (**1j**) [16], (2*E*,4*Z*)-2-cyano-5-(dimethylamino)-*N*,*N*-dimethyl-5-phenylpenta-2,4-dienamide (**1k**) [16], dimethyl (*E*)-2-(3-(dimethylamino)-3-phenylallylidene) malonate (**1l**) [16], (*E*)-4-(benzylsulfonyl)-*N*,*N*,*N*′,*N*″-tetramethyl-4-phenylbuta-1,3-diene-1,1-diamine (**1m**) [21], ethyl (2*Z*,4*E*)-2-cyano-5-(dimethylamino)-3-(*p*-tolyl) penta-2,4-dienoate (**1n**) [20], (*E*)-2-(3-dimethylamino)-1-phenylallylidene)malononitrile (**1o**) [16], (*E*)-2-(5-methyl-1,3,4-thiadiazol-2-yl)-1,3-diphenylprop-2-en-1-one (**1p**) [20], (*E*)-6-(4,4-bi(dimethylamino)-2-methylbuta-1,3-dien-1-yl)-1,3-dimethyl-1,3,5-triazine-2,4(1*H*,3*H*)-dione (**1r**) [21], (*Z*)-2-amino-6,6-bis(dimethylamino)hexa-1,3,5-triene-1,1,3-tricarbonitrile (**1s**) [21], diethyl (*Z*)-(1-cyano-4,4-bis(dimethylamino)buta-1,3-dien-1-yl)phosphonate (**1t**) [22].

4.1 Ethyl 2,3-dimethyl 1-(dimethylamino)-7-oxo-1,7-diphenylhepta-1,3,5-triene-2,3,6-tricarboxylate (2a)

The product was prepared from ethyl 2-benzoyl-5-(dimethylamino)-5-phenylpenta-2,4-dienoate (**1a**, 124 mg,

0.36 mmol) and DMAD (132 µL, 1.07 mmol) in 1.5 mL of acetonitrile, 100°C, 30 min. Column chromatography: ethyl acetate–petroleum ether = 2:3. Yield: 60% (107 mg), red oil. – ^{1}H NMR ($CDCl_3$, 500 MHz): δ = 1.16 (3H, t, J = 7.1 Hz, CH_3), 3.05 (6H, s, $N(CH_3)_2$), 3.66 (3H, s, OCH_3), 3.70 (3H, s, OCH_3), 4.18 (2H, q, J = 7.2 Hz, OCH_2), 6.36 (1H, d, J = 12.5 Hz, CH), 7.29–7.54 (11H, m, 2 Ph and CH). – ^{13}C NMR ($CDCl_3$, 125 MHz): δ = 14.1, 44.1, 51.4, 52.5, 61.4, 96.0, 128.5, 128.6, 128.9, 129.3, 130.3, 130.4, 131.0, 133.3, 133.7, 136.7, 139.2, 142.8, 165.0, 166.2, 166.8, 168.9, 193.4. – HRMS ((+)-EI): m/z = 492.2038 (calcd. 492.2017 for $C_{28}H_{30}NO_7$, $[M+H]^+$). – IR: ν_{max} = 3059, 2981, 2946, 1709, 1668, 1596, 1579, 1528, 1471, 1445, 1432, 1392, 1215, 1166, 1094, 1072, 1023, 932, 766, 754, 690 cm^{-1}.

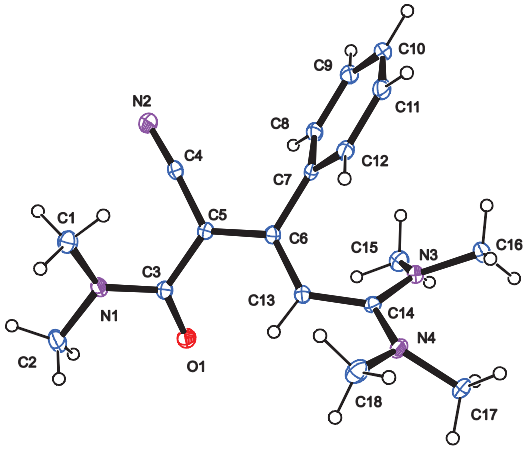

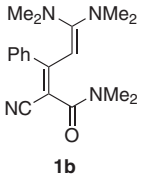

1b

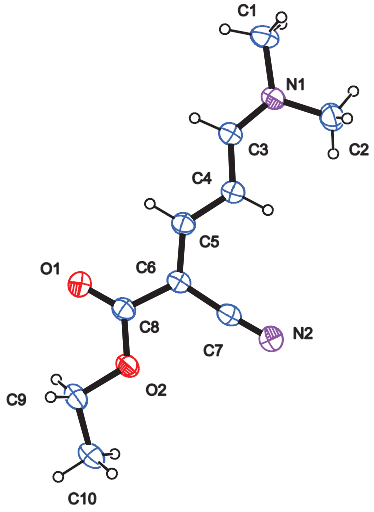

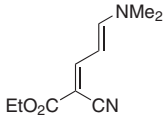

1c

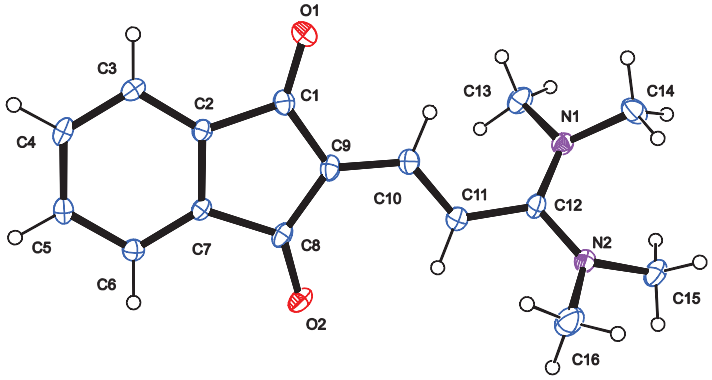

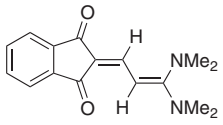

1d

Fig. 6: ORTEP representations of the molecular structures of compounds **1b**, **1c**, **1d**, **1k**, **1l**, and **1g** in the crystal. Displacement ellipsoids are drawn at the 30% probability level; hydrogen atoms as spheres with arbitrary radii.

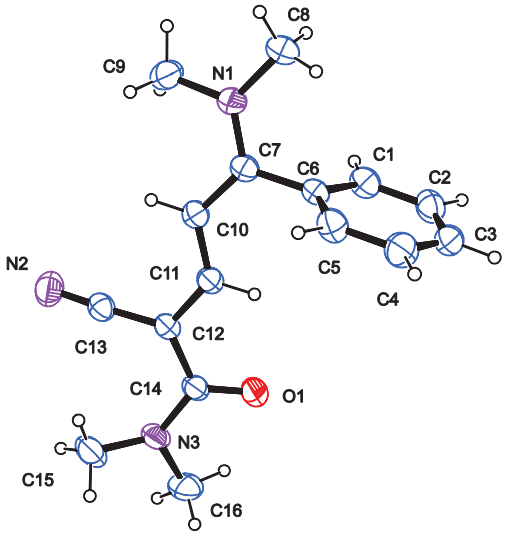

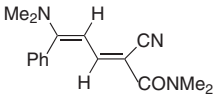

1k

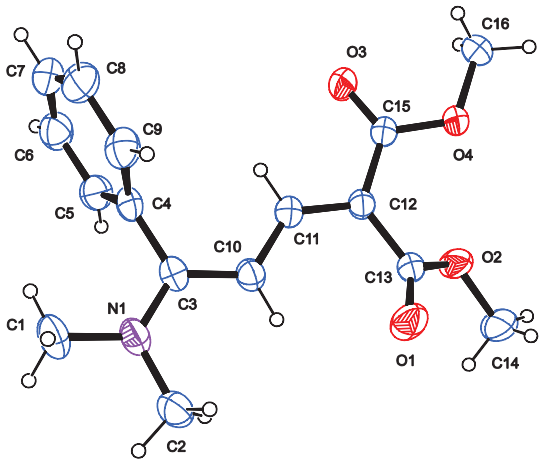

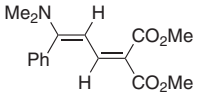

1l

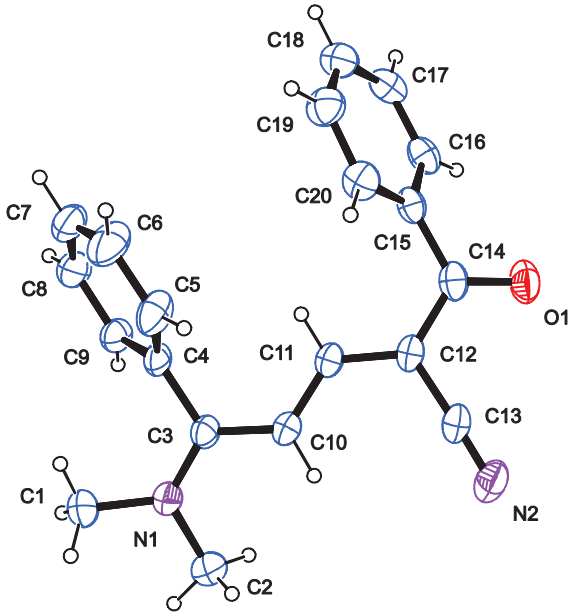

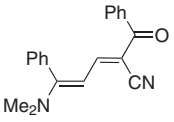

1g

Fig. 6 (continued)

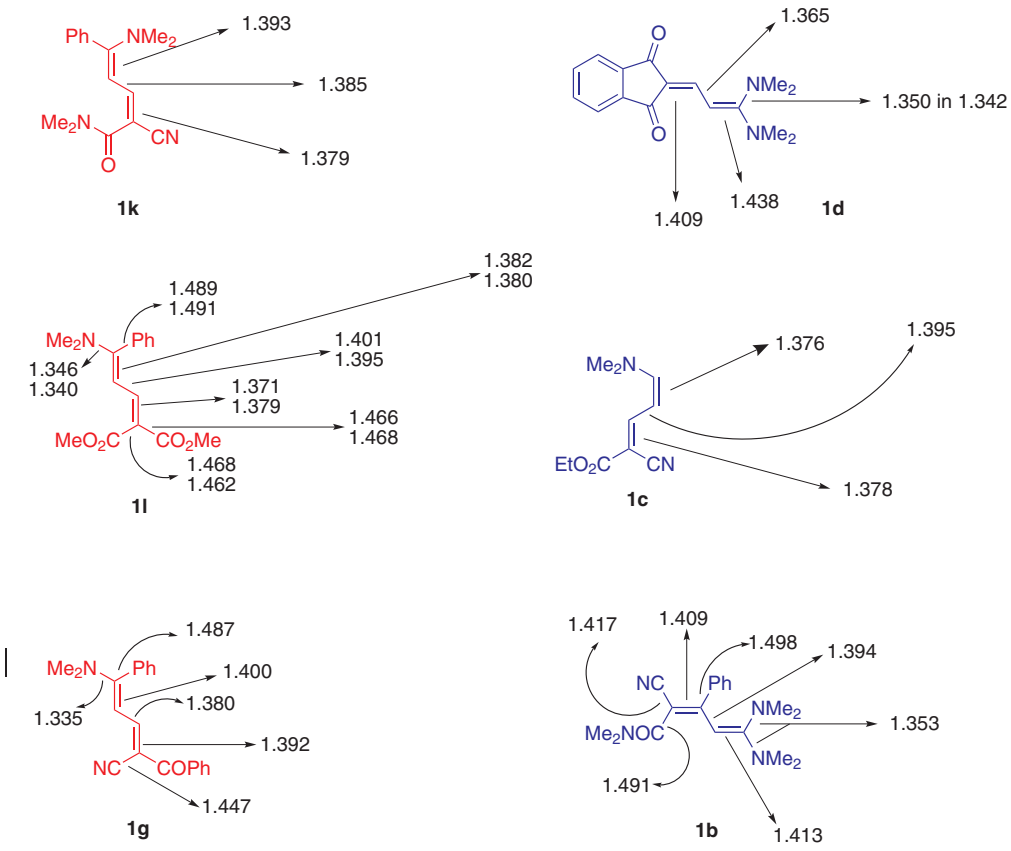

Fig. 7: Bond lengths (in Å) of the single and double bonds of the butadiene structural elements in compounds **1k**, **1l**, and **1g** (unreactive in [2+2] cycloadditions; left, red color) and **1d**, **1c**, and **1b** (reactive in [2+2] cycloadditions; right, blue color) resulting from single-crystal structure determinations.

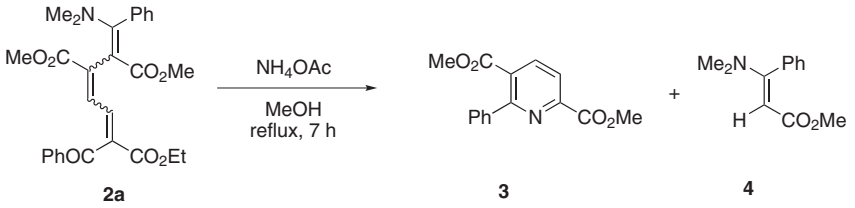

Scheme 3: Formation of dimethyl 2-phenylpyridine-3,6-dicarboxlate (**3**) and methyl 3-amino-3-phenylacrylate (**4**) upon reacting **2a** with ammonium acetate in boiling methanol.

4.2 Dimethyl (*E*)-2-(bis(dimethylamino) methylene)-3-((*Z*)-3-cyano-4-(dimethylamino)-4-oxo-2-phenylbut-2-en-1-ylidene)succinate (2b)

The product was prepared from 2-cyano-5,5-*bis*(dimethylamino)-*N*,*N*-dimethyl-3-phenylpenta-2,4-dieneamide (**1b**, 162 mg, 0.52 mmol) and DMAD (130 µL, 1.04 mmol) in 1.0 mL of acetonitrile, 100°C, 15 min. Column chromatography, ethyl acetate. Yield: 73% (173 mg), red oil. – ^{1}H NMR ($CDCl_3$, 300 MHz): $\delta = 2.28$ (3H, br. s, $N(CH_3)_2$), 2.58 (3H, br. s, $N(CH_3)_2$), 2.69 (3H, br. s, $N(CH_3)_2$), 2.80 (3H, br. s, $N(CH_3)_2$), 2.84 (3H, br. s, $N(CH_3)_2$), 2.89 (3H, br. s, $N(CH_3)_2$), 3.45 (3H, s, OCH_3), 3.75 (3H, s, OCH_3), 6.97 (1H, s, C*H*), 7.23–7.40 (6H, m,

Ph + chloroform). – ^{13}C NMR ($CDCl_3$, 75.5 MHz): δ = 34.6, 35.3, 37.2, 38.2, 39.4, 40.6, 50.6, 52.5, 84.6, 106.2, 116.5, 122.2, 128.6, 128.9, 129.4, 130.4, 135.6, 144.3, 163.3, 167.2, 170.7, 174.2. – HRMS ((+)-EI): *m/z* = 455.2279 (calcd. 455.2289 for $C_{24}H_{31}N_4O_5$, $[M+H]^+$). – IR: ν_{max} = 3011, 2943, 2796, 2247, 2203, 1715, 1671, 1629, 1579, 1532, 1515, 1465, 1447, 1433, 1392, 1329, 1295, 1245, 1229, 1186, 1159, 1118, 1060, 1021, 915, 846, 725, 699 cm^{-1}.

4.3 1-Ethyl 4,5-dimethyl 1-cyano-6-(dimethylamino)hexa-1,3,5-trien-1,4,5-tricarboxylate (2c)

The product was prepared from ethyl 2-cyano-5-(dimethylamino)penta-2,4-dienoate (**1c**, 47 mg, 0.24 mmol) and DMAD (209 µL, 1.70 mmol) in 1 mL of acetonitrile, 100°C, 40 min. Column chromatography, ethyl acetate–petroleum ether = 1:1. Yield: 42% (35 mg), red oil. – ^{1}H NMR ($CDCl_3$, 300 MHz): δ = 1.36 (3H, t, *J* = 7.1 Hz, C*H*$_3$), 2.88 (6H, br. s, N(C*H*$_3$)$_2$), 3.65 (3H, s, OC*H*$_3$), 3.83 (3H, s, OC*H*$_3$), 4.33 (2H, q, *J* = 7.1 Hz, OC*H*$_2$), 7.53 (1H, d, *J* = 12.1 Hz, C*H*), 7.76 (1H, s, C*H*), 7.79 (1H, d, *J* = 12.1 Hz, C*H*). – ^{13}C NMR ($CDCl_3$, 75.5 MHz): δ = 14.2, 43.1, 51.6, 53.0, 62.8, 91.2, 109.2, 113.9, 129.9, 143.7, 150.2, 153.1, 161.7, 167.4, 168.3. – HRMS ((+)-EI): *m/z* = 337.1394 (calcd. 337.1394 for $C_{16}H_{21}N_2O_6$, $[M+H]^+$). – IR: ν_{max} = 2985, 2953, 2848, 2224, 1873, 1718, 1603, 1433, 1232, 1140, 1086, 1041, 1014, 949, 915, 842, 783, 762, 732 cm^{-1}.

4.4 Dimethyl 2-(3,3-bis(dimethylamino) allylidene)-3-(1,3-dioxo-1,3-dihydro-2*H*-indene-2-ylidene)succinate (2d)

The product was prepared from 2-(3,3-*bis*(dimethylamino) allylidene)-1*H*-indene-1,3(2*H*)-dione (**1d**, 32.8 mg, 0.12 mmol) and DMAD (30 µL, 0.24 mmol) in 0.4 mL of acetonitrile, 80°C, 10 min. Column chromatography, ethyl acetate–ethanol = 1:1. Yield: 22% (11 mg), brown oil. – ^{1}H NMR ($CDCl_3$, 500 MHz): δ = 3.11 (12H, s, 2× N(C*H*$_3$)$_2$), 3.70 (3H, s, OC*H*$_3$), 3.87 (3H, s, OC*H*$_3$), 7.34 (1H, d, *J* = 15.1 Hz, C*H*), 7.34 (1H, d, *J* = 15.0 Hz, C*H*), 7.47–7.50 (2H, m, Ph), 7.58–7.61 (2H, m, Ph). – ^{13}C NMR ($CDCl_3$, 125 MHz): δ = 43.0, 51.5, 52.7, 105.5, 110.0, 111.5, 120.7, 132.3, 140.6, 149.1, 152.9, 167.9, 170.7, 171.5, 189.9. – HRMS ((+)-EI): *m/z* = 413.1703 (calcd. 413.1707 for $C_{22}H_{25}N_2O_6$, $[M+H]^+$). – IR: ν_{max} = 3486, 2948, 2925, 2853, 1718, 1614, 1572, 1522, 1488, 1432, 1392, 1336, 1314, 1236, 1191, 1173, 1126, 1056, 964, 914, 891, 773,725, 665 cm^{-1}.

4.5 Diethyl 2-(3,3-bis(dimethylamino) allylidene)-3-(1,3-dioxo-1,3-dihydro-2*H*-indene-2-ylidene)succinate (2e)

The product was prepared from 2-(3,3-*bis*(dimethylamino) allylidene)-1*H*-indene-1,3(2*H*)-dione (**1d**, 62 mg, 0.23 mmol) and DEAD (73 µL, 0.64 mmol) in 0.4 mL of acetonitrile, 75°C, 20 min. Column chromatography, ethyl acetate–ethanol = 1:1. Yield: 44% (45 mg), red-brown oil. – ^{1}H NMR ($CDCl_3$, 500 MHz): δ = 1.24 (3H, t, *J* = 7.1 Hz, C*H*$_3$), 1.33 (3H, t, *J* = 7.1 Hz, C*H*$_3$), 3.12 (12 H, s, N(C*H*$_3$)$_2$), 4.18 (2H, q, *J* = 7.1 Hz, OC*H*$_2$), 4.35 (2J, q, *J* = 7.1 Hz, OC*H*$_2$), 6.10 (1H, d, *J* = 15.0 Hz, C*H*), 7.37 (1H, d, *J* = 15.0 Hz, C*H*), 7.47–7.50 (2H, m, Ph), 7.60–7.63 (2H, m, Ph). – ^{13}C NMR ($CDCl_3$, 125 MHz): δ = 14.2, 14.22, 43.0, 60.3, 61.6, 105.3, 110.3, 111.9, 120.6, 132.3, 140.7, 149.8, 153.6, 167.5, 170.1, 171.7, 189.8. – HRMS ((+)-EI): *m/z* = 441.2022 (calcd. 441.2020 for $C_{24}H_{29}N_2O_6$, $[M+H]^+$). – IR: ν_{max} = 3484, 2978, 2929, 2900, 1723, 1707, 1612, 1572, 1495, 1398, 1361, 1341, 1308, 1231, 1189, 1166, 1123, 1056, 1016, 968, 948, 877, 796, 729, 666 cm^{-1}.

4.6 Dimethyl 2-(3-benzyl-5-methyl-1,3,4-thiadiazol-2(3*H*)-ylidene)-3-(2-oxo-2-phenylethylidene) succinate (2f)

The product was prepared from 2-(3-benzyl-5-methyl-1,3,4-thiadiazol-2(3*H*)-ylidene)-1-phenylethan-1-one (**1e**, 185 mg, 0.60 mmol) and DMAD (148 µL, 1.20 mmol) in 1 mL of acetonitrile, 90 C, 15 min. Column chromatography, ethyl acetate–petroleum ether = 1:3. Yield: 73% (270 mg), red oil. – ^{1}H NMR ($CDCl_3$, 300 MHz): δ = 2.45 (3H, s, C*H*$_3$), 3.42 (3H, s, OC*H*$_3$), 3.59 (3H, s, OC*H*$_3$), 5.11 (1H, br. s, C*H*$_2$), 5.28 (1H, br. s, C*H*$_2$), 6.96–7.00 (2H, m, Ph), 7.19–7.26 (3H, m, Ph), 7.40–7.46 (2H, m, Ph), 7.53–7.58 (1H, m, Ph), 7.78 (1H, s, C*H*), 7.84–7.88 (2H, m, Ph). – ^{13}C NMR ($CDCl_3$, 75.5 MHz): δ = 15.3, 51.6, 52.7, 56.2, 83.7, 126.8, 127.2, 127.7, 128.5, 128.6, 131.7, 133.4, 135.5, 136.9, 137.4, 152.7, 161.3, 167.7, 167.9, 191.7. – HRMS ((+)-EI): *m/z* = 451.1327 (calcd. 451.1322 for $C_{24}H_{23}N_2O_5S$, $[M+H]^+$). – IR: ν_{max} = 3030, 2993, 2944, 2833, 1716, 1654, 1594, 1583, 1494, 1449, 1427, 1317, 1247, 1183, 1107, 1043, 1013, 983, 941, 891, 865, 796, 739, 697 cm^{-1}.

4.7 Dimethyl 2-(3,5-dimethyl-1,3,4-tiadiazol-2(3*H*)-ylidene)-3-(2-(4-methoxyphenyl)-2-oxoethylidene)succinate (2g)

The product was prepared from 2-(3,5-dimethyl-1,3,4-thiadiazol-2(3*H*)-ylidene)-1-(4-methoxyphenyl)ethan-1-one

(**1f**, 187 mg, 0.71 mmol) and DMAD (175 µL, 1.43 mmol) in 1 mL of acetonitrile, 100°C, 15 min. Column chromatography, ethyl acetate–petroleum ether = 2:3. Yield: 65% (186 mg), red oil. – ^{1}H NMR ($CDCl_3$, 300 MHz): δ = 2.40 (3H, s, CH_3), 3.46 (3H, s, NCH_3), 3.65 (3H, s, OCH_3), 3.84 (3H, s, OCH_3), 3.85 (3H, s, OCH_3), 6.85–6.90 (2H, m, Ph), 7.55 (1H, s, C*H*), 7.81–7.86 (2H, m, Ph). – ^{13}C NMR ($CDCl_3$, 75.5 MHz): δ = 15.2, 41.5, 51.5, 52.9, 55.5, 82.5, 113.8, 130.1, 130.2, 130.8, 136.6, 152.7, 162.5, 163.7, 167.5, 169.1, 190.0. – HRMS ((+)-EI): *m/z* = 405.1120 (calcd. 405.1115 for $C_{19}H_{21}N_2O_6S$, $[M+H]^+$). – IR: ν_{max} = 2994, 2948, 2840, 1719, 1649, 1595, 1573, 1494, 1432, 1306, 1280, 1248, 1226, 1164, 1133, 1059, 1020, 979, 960, 911, 876, 726, 699 cm^{-1}.

4.8 Dimethyl 2-phenylpyridine-3, 6-dicarboxylate (3)

The product was prepared from 6-ethyl 2,3-dimethyl 1-(dimethylamino)-7-oxo-1,7-diphenylhepta-1,3,5-trien-2,3,6-tricarboxylate (**2a**, 90.0 mg, 0.18 mmol) and ammonium acetate (566 mg, 7.34 mmol) in 7 mL of methanol, heating at reflux temperature for 7 h, and then stirring at room temperature overnight. Volatile components were removed under reduced pressure. The product was isolated from the crude residue with flash chromatography. A mixture of ethyl acetate–petroleum ether (2:1) was used as the eluent. Yield: 58% (29 mg), brown oil. – ^{1}H NMR ($CDCl_3$, 500 MHz): δ = 3.76 (3H, s, OCH_3), 3.96 (3H, s, OCH_3), 7.43–7.47 (3H, m, Ph), 7.59–7.63 (2H, m, Ph), 7.77 (1H, d, *J* = 5.0 Hz, 5-C*H*), 8.87 (1H, d, *J* = 5.0 Hz, 4-C*H*). – ^{13}C NMR ($CDCl_3$, 125 MHz): δ = 52.9, 53.3, 121.3, 128.5, 128.6, 129.0, 129.3, 136.5, 138.8, 150.8, 157.6, 165.1, 168.4. – HRMS ((+)-EI): *m/z* = 272.0926 (calcd. 272.0917 for $C_{15}H_{13}NO_4$, $[M+H]^+$). – IR: ν_{max} = 2996, 2950, 2847, 1730, 1663, 1618, 1558, 1492, 1460, 1433, 1399, 1310, 1279, 1257, 1202, 1171, 1124, 1079, 1060, 1026, 969, 854, 806, 772, 751, 739, 700 cm^{-1}.

4.9 Methyl 3-amino-3-phenylakrylate (4) [23]

This compound [23] was formed and isolated as the side product in preparation of compound **3**.

4.10 Crystal structure determinations of compounds 1b, 1c, 1d, 1g, 1k, 1l, and 2b

An Agilent SuperNova diffractometer equipped with an Atlas detector was used for the single-crystal structure determinations of the aforementioned compounds. Diffraction data of single crystals of compounds **1b** and **1d** were collected at *T* = 150 K, whereas diffraction data for all other structures were collected at room temperature. Cu*K*α radiation (*λ* = 1.54184 Å) was used for the data collection of **2b**, whereas Mo*K*α radiation (*λ* = 0.71073 Å) was used for all other compounds. Data reduction and integration were performed with the software package CrysAlis Pro [24]. All structures were solved by Direct Methods with the programs Sir97 [25, 26] or Olex2 structure solution program [27]. Full-matrix least-squares refinements on F^2 were done with anisotropic displacement parameters for all nonhydrogen atoms using Shelxl-2014/7 [28, 29]. All hydrogen atoms were initially located in difference Fourier maps. Carbon-attached hydrogens were subsequently treated as riding atoms in geometrically idealized positions with bond lengths C–H of 0.96/0.98 Å for methyl and 0.93/0.95 Å for aromatic C–H bonds (the first values refer to room temperature and the second to low temperature). The corresponding displacement parameters U_{iso}(H) were set 1.5 times higher than those of the carrier methyl carbons and 1.2 times higher than aromatic carbon atoms. Figures depicting the structures were prepared with Ortep-III [30–32].

4.11 Crystallographic data

For **1b**: $C_{18}H_{24}N_4O$, M_r = 312.41, yellow prisms, 0.20 × 0.20 × 0.10 mm^3, triclinic, space group $P\bar{1}$ (no. 2), *a* = 10.0400(6) Å, *b* = 10.3977(7) Å, *c* = 10.6856(4) Å, *α* = 60.978(5)°, *β* = 73.151(4)°, *γ* = 62.068(6)°, *V* = 858.96(10) Å^3, *Z* = 2, D_x = 1.208 Mg m^{-3}, *F*(000) = 336 *e*, *μ* = 0.078 mm^{-1}, *T* = 150(2) K, Mo*K*α radiation, *ω* scans, *θ* range: 3.046–30.336°; *hkl* range: –13 ≤ *h* ≤ 11, –14 ≤ *k* ≤ 13, –14 ≤ *l* ≤ 14; 7654 measured, 4438 independent and 3453 observed reflections, R_{int} = 0.0220, multiscan absorption correction, refinement on F^2, $R(F)$ [$F^2 > 2\,\sigma(F^2)$] = 0.0461, $wR(F^2)$ (all data) = 0.1151, 4438 contributing reflections, 214 ref. parameters, 0 restraints, Shelxl-2014/7 weighting scheme, $\Delta\rho_{max}$ = 0.298 *e* Å^{-3}, $\Delta\rho_{min}$ = –0.192 *e* Å^{-3}.

For **1c**: $C_{10}H_{14}N_2O_2$, M_r = 194.23, colorless platelets, 0.30 × 0.20 × 0.10 mm^3, monoclinic, space group $P2_1/n$ (no. 14), *a* = 6.6196(4) Å, *b* = 8.7859(4) Å, *c* = 18.3836(10) Å, *β* = 92.894(5)°, *V* = 1067.81(10) Å^3, *Z* = 4, D_x = 1.208 Mg m^{-3}, *F*(000) = 416 *e*, *μ* = 0.085 mm^{-1}, *T* = 293(2) K, Mo*K*α radiation, *ω* scans, θ range: 3.209–30.415°; *hkl* range: –8 ≤ *h* ≤ 9, –11 ≤ *k* ≤ 12, –25 ≤ *l* ≤ 23; 9230 measured, 2901 independent and 2101 observed reflections, R_{int} = 0.0284, multiscan absorption correction, refinement on F^2, $R(F)$ [$F^2 > 2\,\sigma(F^2)$] = 0.0786, $wR(F^2)$ (all data) = 0.2428, 2901

contributing reflections, 130 parameters, 0 restraints, SHELXL-2014/7 weighting scheme, $\Delta\rho_{max} = 0.260$ *e* Å^{-3}, $\Delta\rho_{min} = -0.200$ *e* Å^{-3}.

For **1d**: $C_{16}H_{18}N_2O_2$, $M_r = 270.32$, brown prisms, $0.40 \times 0.20 \times 0.15$ mm^3, monoclinic, space group $P2_1/c$ (no. 14), $a = 9.7114(3)$ Å, $b = 11.7763(3)$ Å, $c = 13.0242(4)$ Å, $\beta = 109.030(4)°$, $V = 1408.10(8)$ Å^3, $Z = 4$, $D_x = 1.275$ Mg m^{-3}, $F(000) = 576$ *e*, $\mu = 0.085$ mm^{-1}, $T = 150(2)$ K, Mo*K*α radiation, ω scans, θ range: 2.813–30.334°; *hkl* range: $-8 \le h \le 13$, $-16 \le k \le 16$, $-17 \le l \le 18$; 8719 measured, 3700 independent and 2833 observed reflections, $R_{int} = 0.0243$, multiscan absorption correction, refinement on F^2, $R(F)$ $[F^2 > 2\ \sigma(F^2)] = 0.0720$, $wR(F^2)$ (all data) = 0.2054, 3700 contributing reflections, 185 parameters, 0 restraints, SHELXL-2014/7 weighting scheme, $\Delta\rho_{max} = 0.962$ *e* Å^{-3}, $\Delta\rho_{min} = -0.352$ *e* Å^{-3}.

For **1g**: $C_{20}H_{18}N_2O$, $M_r = 302.36$, orange prisms, $0.45 \times 0.25 \times 0.20$ mm^3, monoclinic, space group $P2_1/n$ (no. 14), $a = 9.6203(3)$ Å, $b = 17.7657(7)$ Å, $c = 9.9957(4)$ Å, $\beta = 95.113(3)°$, $V = 1701.58(11)$ Å^3, $Z = 4$, $D_x = 1.180$ Mg m^{-3}, $F(000) = 640$ *e*, $\mu = 0.074$ mm^{-1}, $T = 293(2)$ K, Mo*K*α radiation, ω scans, θ range: 2.816–30.417°; *hkl* range: $-13 \le h \le 12$, $-23 \le k \le 24$, $-12 \le l \le 13$; 17784 measured, 4623 independent and 3031 observed reflections, $R_{int} = 0.0254$, multiscan absorption correction, refinement on F^2, $R(F)$ $[F^2 > 2\ \sigma(F^2)] = 0.0568$, $wR(F^2)$ (all data) = 0.1841, 4623 contributing reflections, 210 parameters, 0 restraints, SHELXL-2014/7 weighting scheme, $\Delta\rho_{max} = 0.163$ *e* Å^{-3}, $\Delta\rho_{min} = -0.163$ *e* Å^{-3}.

For **1k**: $C_{16}H_{19}N_3O$, $M_r = 269.34$, yellow prisms, $0.35 \times 0.15 \times 0.15$ mm^3, monoclinic, space group $P2_1/c$ (no. 14), $a = 10.4687(6)$ Å, $b = 14.2688(6)$ Å, $c = 11.3323(5)$ Å, $\beta = 114.632(6)°$, $V = 1538.72(15)$ Å^3, $Z = 4$, $D_x = 1.163$ Mg m^{-3}, $F(000) = 576$ *e*, $\mu = 0.075$ mm^{-1}, $T = 293(2)$ K, Mo*K*α radiation, ω scans, θ range: 2.855–30.439°; *hkl* range: $-13 \le h \le 14$, $-19 \le k \le 13$, $-14 \le l \le 11$; 8957 measured, 4015 independent and 2484 observed reflections, $R_{int} = 0.0222$, multiscan absorption correction, refinement on F^2, $R(F)$ $[F^2 > 2\ \sigma(F^2)] = 0.0579$, $wR(F^2)$ (all data) = 0.1679, 4015 contributing reflections, 185 parameters, 0 restraints, SHELXL-2014/7 weighting scheme, $\Delta\rho_{max} = 0.161$ *e* Å^{-3}, $\Delta\rho_{min} = -0.160$ *e* Å^{-3}.

For **1l**: $C_{16}H_{19}NO_4$, $M_r = 289.32$, yellow prisms, $0.45 \times 0.25 \times 0.15$ mm^3, monoclinic, space group $P2_1/n$ (no. 14), $a = 11.1211(2)$ Å, $b = 14.7658(3)$ Å, $c = 19.4274(4)$ Å, $\beta = 93.547(2)°$, $V = 3184.10(11)$ Å^3, $Z = 8$, $D_x = 1.207$ Mg m^{-3}, $F(000) = 1232$ *e*, $\mu = 0.087$ mm^{-1}, $T = 293(2)$ K, Mo*K*α radiation, ω scans, θ range: 2.952–30.445°; *hkl* range: $-15 \le h \le 13$, $-20 \le k \le 18$, $-25 \le l \le 27$; 35943 measured, 8856 independent and 5611 observed reflections, $R_{int} = 0.0260$, multiscan absorption correction, refinement on F^2, $R(F)$ $[F^2 > 2\ \sigma(F^2)] = 0.0567$, $wR(F^2)$ (all data) = 0.1691, 8856 contributing reflections, 387 parameters, 0 restraints, SHELXL-2014/7 weighting scheme, $\Delta\rho_{max} = 0.296$ *e* Å^{-3}, $\Delta\rho_{min} = -0.221$ *e* Å^{-3}.

For **2b** · $CHCl_3$: $C_{24}H_{30}N_4O_5 \cdot CHCl_3$, $M_r = 573.89$, red platelets, $0.25 \times 0.25 \times 0.08$ mm^3, monoclinic, space group $P2_1$ (no. 4), $a = 11.1105(6)$ Å, $b = 10.3368(6)$ Å, $c = 13.3025(7)$ Å, $\beta = 107.939(6)°$, $V = 1453.48(15)$ Å^3, $Z = 2$, $D_x = 1.311$ Mg m^{-3}, $F(000) = 600$ *e*, $\mu = 3.192$ mm^{-1}, $T = 293(2)$ K, Cu*K*α radiation, ω scans, θ range: 4.182–74.486°; *hkl* range: $-11 \le h \le 13$, $-8 \le k \le 12$, $-16 \le l \le 16$; 8314 measured, 4072 independent and 3686 observed reflections, $R_{int} = 0.0323$, multiscan absorption correction, refinement on F^2, $R(F)$ $[F^2 > 2\,\sigma(F^2)] = 0.0498$, $wR(F^2)$ (all data) = 0.1477, Flack $(x) = 0.045(16)$, 4072 contributing reflections, 341 parameters, 1 restraint, SHELXL-2014/7 weighting scheme, $\Delta\rho_{max} = 0.360$ *e* Å^{-3}, $\Delta\rho_{min} = -0.338$ *e* Å^{-3}. As the only compound of this series, **2b** crystallizes as a solvate with one molecule of $CHCl_3$ per formula unit.

CCDC 1835675–1835681 contain the supplementary crystallographic data for this paper. These data can be obtained free of charge from The Cambridge Crystallographic Data Centre via www.ccdc.cam.ac.uk/data_request/cif.

Acknowledgment: We are grateful for the financial support from the Slovenian Research Agency, Slovenia, through grants P1-0175 and P1-0179. We acknowledge with thanks the financial support from the pharmaceutical company KRKA, d.d., Novo mesto, Slovenia. We thank EN-FIST Centre of Excellence, Trg OF 13, 1000 Ljubljana, Slovenia, for using the SuperNova diffractometer.

References

[1] B. Stanovnik, *Org. Prep. Proced. Int.* **2014**, *46*, 24.
[2] J. Bezenšek, T. Koleša, U. Grošelj, A. Meden, K. Stare, J. Svete, B. Stanovnik, *Curr. Org. Chem.* **2011**, *15*, 2530.
[3] J. Bezenšek, T. Koleša, U. Grošelj, J. Wagger, K. Stare, A. Meden, J. Svete, B. Stanovnik, *Tetrahedron Lett.* **2010**, *51*, 3392.
[4] F. Bohlmann, D. Rahtz, *Chem. Ber.* **1957**, *90*, 2265.
[5] M. C. Bagley, J. W. Dale, J. Bower, *Synlett* **2001**, 1149.
[6] J. Bezenšek, B. Prek, U. Grošelj, M. Kasunič, J. Svete, B. Stanovnik, *Tetrahedron* **2012**, *68*, 4719.
[7] G. Maas, B. Singer, P. Wald, M. Gimmy, *Chem. Ber.* **1988**, *121*, 1847.
[8] R. Rahm, G. Maas, *Chem. Ber.* **1994**, *127*, 1295.
[9] K. Drandarov, I. Tiritiris, O. Wassiljew, H.-U. Siehl, W. Kantlehner, *Chem. Eur. J.* **2011**, *18*, 7224.

[10] J. Bezenšek, B. Prek, U. Grošelj, A. Golobič, K. Stare, J. Svete, W. Kantlehner, G. Maas, B. Stanovnik, *Z. Naturforsch*. **2014**, *69b*, 554.
[11] B. Prek, J. Bezenšek, M. Kasunič, U. Grošelj, J. Svete, B. Stanovnik, *Tetrahedron* **2014**, *70*, 2359.
[12] B. Prek, U. Grošelj, M. Kasunič, S. Zupančič, J. Svete, B. Stanovnik, *Aust. J. Chem.* **2015**, *68*, 184.
[13] B. Prek, J. Bezenšek, B. Stanovnik, *Tetrahedron* **2017**, *73*, 5260, and references cited therein.
[14] J. Bezenšek, B. Prek, U. Grošelj, M. Počkaj, J. Svete, B. Stanovnik, *Tetrahedron* **2015**, *71*, 7209.
[15] J. Bezenšek, U. Grošelj, M. Počkaj, J. Svete, B. Stanovnik, *Tetrahedron Lett*. **2015**, *56*, 5705.
[16] M. Kiesel, E. Haug, W. Kantlehner, *J. Prakt. Chem*. **1997**, *339*, 159–170.
[17] W. Kantlehner, M. Vettel, H. Lehmann, K. Edelmann, R. Stieglitz, I. C. Ivanov, *J. Prakt. Chem*. **1998**, *340*, 408.
[18] K. Edelmann, *Dissertation*, Universität Stuttgart, Stuttgart, **1998**, p. 103.
[19] K. Edelmann, *Dissertation*, Universität Stuttgart, Stuttgart, **1998**, p.104.
[20] W. Kantlehner, H. Lehmann, T. Stahl, W. Kaim, *Chem. Ztg*. **1991**, *115*, 183.
[21] J. Mezger, *Dissertation*, Universität Stuttgart, Stuttgart, **2002**, p. 173.
[22] H. Lehmann, *Dissertation*, Universität Stuttgart, Stuttgart, **1991**, p. 14.
[23] T. Sasada, F. Kobayashi, N. Sakai, T. Konakahara, *Org. Lett*. **2009**, *11*, 2161.
[24] CrysAlis Pro Software System, Intelligent Data Collection and Processing Software for Small Molecule and Protein Crystallography, Agilent Technologies Ltd., Yarnton, Oxfordshire (UK), **2011**.
[25] A. Altomare, M. C. Burla, M. Camalli, G. L. Cascarano, C. Giacovazzo, A. Guagliardi, A. G. G. Moliterni, G. Polidori, R. Spagna, Sir97, *A New Tool for Crystal Structure Determination and Refinement*, Bari, Perugia, Rome (Italy), **1997**.
[26] A. Altomare, M. C. Burla, M. Camalli, G. L. Cascarano, C. Giacovazzo, A. Guagliardi, A. G. G. Moliterni, G. Polidori, R. Spagna, *J. Appl. Crystallogr*. **1999**, *32*, 115.
[27] L. J. Bourhis, O. V. Dolomanov, R. J. Gildea, J. A. K. Howard, H. Puschmann, *Acta Crystallogr.* **2015**, *A71*, 59.
[28] G. M. Sheldrick, Shelxl-2014/7, *Program for the Refinement of Crystal Structures*, University of Göttingen, Göttingen (Germany), **2013**.
[29] G. M. Sheldrick, *Acta Crystallogr.* **2015**, *C71*, 3.
[30] C. K. Johnson, M. N. Burnett, Ortep-III (version 1.0.2), Oak Ridge Thermal Ellipsoid Plot Program for Crystal Structure Illustrations, Rep. ORNL-6895, Oak Ridge National Laboratory, Oak Ridge, TN (USA), **1996**.
[31] Windows version: L. J. Farrugia, University of Glasgow, Glasgow, Scotland (UK), **1999**.
[32] L. J. Farrugia, *J. Appl. Crystallogr.* **2012**, *45*, 849.